N-phenethylphenazine-1-carboxamide, a Novel Antiviral Compound Against Infectious Bronchitis Virus

Zhichao Cai , Mingjing Zhang , Junkai Li , Qinglai Wu , Dingxiang Liu * , Shouguo Fang *

Posted Date: 14 March 2025

doi: 10.20944/preprints202503.1058.v1

Keywords: *N*-phenethylphenazine-1-carboxamide; infectious bronchitis virus; antiviral activity

Article

N-phenethylphenazine-1-carboxamide, a Novel Antiviral Compound Against Infectious Bronchitis Virus

Zhichao Cai [1], Mingjing Zhang [1], Junkai Li [1], Qinglai Wu [1], Dingxiang Liu [2,3,*] and Shouguo Fang [1,*]

[1] College of Agriculture, Yangtze University, Jingzhou 434025, China

[2] Zhaoqing Branch Centre of Guangdong Laboratory for Lingnan Modern Agricultural Science and Technology, Zhaoqing 526238, China

[3] Integrative Microbiology Research Centre, South China Agricultural University, Guangzhou 510642, China

* Correspondence: dxliu0001@163.com (D.L.); sg-fang@hotmail.com (S.F.)

Abstract: Avian infectious bronchitis virus (IBV) is a globally prevalent, highly contagious avian pathogen that imposes substantial disease burden and economic losses on the poultry industry. Due to the challenges associated with vaccine immunization, there is an urgent need to develop novel anti-IBV therapeutic strategies. In this study, a synthesized novel compound N-phenethylphenazine-1-carboxamide (SQXA-12) was investigated for its significant inhibitory effects on IBV replication. SQXA-12 exhibited low cytotoxicity and high antiviral efficacy, with a CC_{50} value of 122.98 μM and an EC_{50} value of 12.25 μM. Sensitivity tests against VSV, HCoV-OC43, PEDV, NDV, PRRSV, and AIV-H9N2 revealed that SQXA-12 possesses potential broad-spectrum antiviral activity against both positive- and negative-sense RNA viruses. These findings highlight the promising therapeutic potential of SQXA-12 for IBV infection.

Keywords: *N*-phenethylphenazine-1-carboxamide; infectious bronchitis virus; antiviral activity

1. Introduction

Coronavirus is a positive-sense single-stranded RNA virus that can infect numerous mammalian species, including humans, posing significant threats to public health and causing substantial economic losses [1]. Avian infectious bronchitis virus (IBV), which belongs to the genus Gamma-coronavirus, primarily infects the respiratory tract, kidneys, and reproductive organs and tissues of chickens, thereby severely impeding the sustainable development of the poultry industry [2]. Currently, inactivated or attenuated vaccines are predominantly employed in the prevention and control of IBV-induced diseases. However, due to the high mutation rate and genetic recombination of IBV, diverse serotypes and pathogenic variants have emerged, leading to suboptimal immune responses or even immunity failure [3–5]. Although several therapeutic drugs, including Nirmatrelvir/ritonavir, molnupiravir, azvudine, etc, have been authorized for treating patients with COVID-19 [6–10], their efficacy against IBV has not been documented. Therefore, the screening and research and development of safe and efficacious novel anti-IBV drugs hold significant potential for practical application.

Phenazine compounds are a class of aromatic compounds with redox properties. Mainly included phenazine-1-carboxylic acid (PCA), phenazine-1-carboxamide (PCN) and 2-hydroxyphenazine-1-carboxylic acid (2-OH-PCA). These compounds are secondary metabolites produced by *Pseudomonas spp*. and *Streptomyces spp.*, and exhibit broad-spectrum antimicrobial activity against a variety of plant pathogenic fungi, oomycetes, and bacteria [11,12]. Several PCA amide analogues exhibit notable antifungal activities [13]. However, antiviral studies remain limited, with only two PCA amide derivatives reported to exhibit inhibitory activity against T7 bacteriophage and bovine viral diarrhea virus [14].

 doi:10.20944/preprints202503.1058.v1

In this study, we identified the PCA amide compound N-phenethylphenazine-1-carboxamide (SQXA-12), which exhibits in vitro inhibitory activity against IBV Beaudette strain and IBV-M41 in chicken embryo. Moreover, it showed comparable inhibitory effects on vesicular stomatitis virus (VSV), human coronavirus OC43 (HCoV-OC43), porcine epidemic diarrhea virus (PEDV), Newcastle disease virus (NDV), porcine reproductive and respiratory syndrome virus (PRRSV), and avian influenza virus H9N2 (AIV-H9N2). These findings suggest that SQXA-12 holds significant potential as an antiviral agent for the clinical management and prevention of outbreaks involving IBV and other RNA viruses.

2. Materials and Methods

2.1. Cell Lines, Viruses, and Compounds

Marc-145 cells were generously provided by Dr. Ding Xiang Liu from the Zhaoqing Branch Center of Guangdong Laboratory for Lingnan Modern Agricultural Science and Technology. Vero, Marc-145, and DF-1 cells were maintained in Dulbecco's Modified Eagle's Medium (DMEM) (Gibco, USA), while H1299 cells were cultured in RPMI 1640 medium (Gibco, USA). All culture media were supplemented with 10% fetal bovine serum (FBS) (Gibco, USA), 100 units/mL penicillin, and 100 units/mL streptomycin (Invitrogen, USA). IBV Beaudette strain IBV-p65 (GenBank accession number DQ001339.1) and a recombinant virus rIBV, based on the IBV-p65 sequence [15], were used as the wild-type virus. IBV-Luc is a recombinant virus in which the open reading frame (ORF) 3a-3b is replaced with the firefly luciferase gene [16]. HCoV-OC43, PEDV, NDV, PRRSV, and AIV-H9N2 were generously provided by Dr. Ding Xiang Liu. GFP-VSV was kindly supplied by Dr. Changjiang Weng from the Harbin Veterinary Research Institute, Chinese Academy of Agricultural Sciences. IBV-p65 and IBV-Luc were propagated in Vero cells, while IBV-M41 was propagated in chicken embryos. PCA and SQXA-12 ($C_{21}H_{17}N_3O$, molecular mass: 327.38) were provided by Prof. Junkai Li from the Agricultural College of Yangtze University and were dissolved in dimethyl sulfoxide (DMSO) (Solarbio, China). 2-Phenethylamine was obtained from Macklin (China).

2.2. Antibodies

The anti-IBV-N polyclonal antibody was prepared and stored in our laboratory. The anti-GAPDH antibody (ab181603) was sourced from Abcam (United Kingdom). Anti-β-actin (AC026) and HRP goat anti-rabbit IgG (AS014) antibodies were obtained from ABclonal Technology (China). Additionally, the anti-HCoV-OC43-N, anti-PEDV-N, anti-NDV, and anti-PRRSV-N antibodies were kindly provided by Professor Ding Xiang Liu.

2.3. Methyl Thiazolyl Tetrazolium (MTT) Assay

The cytotoxicity of SQXA-12 on Vero cells was assessed using the MTT assay. Vero cells were seeded in 24-well plates and cultured until they reached approximately 50% confluence, at which point they were exposed to varying concentrations of SQXA-12. The treatment period was terminated when the control group achieved 90% confluence. Subsequently, the culture medium was replaced with serum-free DMEM, and the cells were incubated with a 0.5% MTT solution for 4 hours. Following this incubation, the supernatant was aspirated from each well, and 1 mL of DMSO was added to dissolve the formazan crystals. The optical density of each well was measured at 490 nm using a Sense microplate reader (Hidex, Finland). The experimental data were analyzed to determine the 50% cytotoxic concentration (CC_{50}) of SQXA-12 using GraphPad Prism 8.0.

2.4. Luciferase Reporter Assay

Vero cells, cultured to 90% confluence in 12-well plates, were inoculated with IBV-Luc at a multiplicity of infection (MOI) of 1.0 for 2 hours. Subsequently, the culture medium was replaced with serum-free DMEM. Concurrently, cells were exposed to varying concentrations of SQXA-12 or an equivalent volume of DMSO as a control. At 24 hours post-infection, cells were harvested for

 doi:10.20944/preprints202503.1058.v1

luciferase activity measurement. The luciferase reporter assay was conducted according to the manufacturer's instructions (Promega, USA). Relative fluorescence units (RLUs) were quantified using a GloMax 20/20 luminometer (Promega, USA). Data obtained from these experiments were analyzed to determine the 50% effective concentration (EC_{50}) of SQXA-12 using GraphPad Prism 8.0.

2.5. Virus Growth Curves

To characterize the growth kinetics of IBV in H1299 cells, a plaque assay was conducted following a standardized protocol using Vero cells as the host. H1299 cells were inoculated with recombinant IBV (rIBV) at a multiplicity of infection (MOI) of 1.0. At 2 hours post-infection (hpi), the culture medium was replaced with serum-free DMEM supplemented with 12.25 μM SQXA-12. Cell lysates and supernatants were collected at 2, 4, 8, 16, 24, and 36 hpi for subsequent analysis. The plaques were quantified in Vero cells via plaque assay, and average viral titers were determined from triplicate samples.

2.6. RT-qPCR Determination of Viral and Cellular RNAs

Total RNA was extracted from each treated cell sample using the Trizol reagent and subsequently utilized as templates for reverse transcription (RT) with the HiScript II First Strand cDNA Synthesis Kit (+gDNA wiper) (Vazyme, China). RT-qPCR analysis was conducted using ChamQ Universal SYBR qPCR Master Mix (Vazyme, China). The thermal cycling conditions were as follows: initial denaturation at 95 °C for 30 seconds, followed by 40 cycles of denaturation at 95 °C for 10 seconds and annealing/extension at 60 °C for 30 seconds. The primer sequences used were as follows: for IBV negative genomic RNA, forward 5′-TGAAGGTAGCGGTGTTCCTG-3′ and reverse 5′-CCACGGTTCAGGGGAATGAA-3′; for IBV subgenomic RNA, forward 5′-CTATTATACTAGCCTTGCGCT-3′ and reverse 5′-GTTAACTACCGCATAAGCACC-3′; for Homo GAPDH, forward 5′-GTCAAGGCTGAGAACGGGAA-3′ and reverse 5′-AGTGATGGCATGGACTGTGG-3′. These primers were employed to quantify the relative expression levels of viral and cellular RNAs. The relative expression levels were determined using the $2^{-\Delta\Delta Ct}$ method, with GAPDH serving as the reference gene. All experiments were performed in triplicate. Statistical analysis and data visualization were carried out using GraphPad Prism 8.0.

2.7. Western Blotting

The Western blotting experiment was conducted following a previously published protocol [17] with minor modifications. Total protein from each cell sample was extracted using RIPA buffer (Solarbio, China) supplemented with 1 mM PMSF (Solarbio, China). The extracted proteins were mixed with loading buffer, denatured by boiling at 100°C for 5 minutes, and clarified through centrifugation. Protein separation was achieved via SDS-PAGE, followed by transfer to a polyvinylidene difluoride (PVDF) membrane (Millipore, USA). The membrane was blocked for 2 hours at room temperature in blocking buffer (5% fat-free milk powder in TBS buffer containing 0.1% Tween 20 (TBST)), then incubated overnight at 4°C with primary antibodies diluted in TBST. Following three washes with TBST, the membrane was incubated with HRP-conjugated goat anti-rabbit IgG secondary antibody in TBST for 2 hours at room temperature. After additional washes with TBST, protein bands were visualized using an ECL chemiluminescence detection kit (Thermo, USA) according to the manufacturer's instructions. The resulting blots were exposed for imaging.

2.8. Chick Embryo Test

Five-day-old specific pathogen-free (SPF) chicken embryos were incubated at 37°C for several days. Daily candling was conducted to monitor embryo viability, and any embryos exhibiting detached blood vessels were excluded from the study. On day 10, an aperture was carefully created in the air sac to facilitate drug administration. On day 12, this procedure was repeated for both drug and virus administration. Each embryo received an inoculation of 200 μL of solution, after which the

 doi:10.20944/preprints202503.1058.v1

injection site was sealed with melted wax. The embryos were then returned to the incubator at 37°C until they reached the desired developmental stage. Following this, the embryos were transferred to a 4°C environment overnight to promote blood coagulation. Subsequently, embryo growth was evaluated, or allantoic fluid was harvested as required. All remaining materials were subjected to high-temperature and high-pressure decontamination prior to disposal.

2.9. Hemagglutination Test

Freshly collected chicken erythrocytes were resuspended in PBS, subjected to centrifugation at 150 g for 5 minutes, and washed three times with PBS. A 1% erythrocyte suspension was prepared in PBS and stored at 4°C until further use. For the hemagglutination assay, a 96-well U-bottom plate was employed. Each well received 25 μL of PBS. The test sample (25 μL) was added to the first well, mixed thoroughly, and serial two-fold dilutions were performed by transferring 25 μL to subsequent wells. Thereafter, 25 μL of the pre-mixed 1% erythrocyte suspension was added to each well, followed by incubation at 37°C for 20 minutes. Post-incubation, the plate was examined vertically to evaluate hemagglutination activity.

2.10. Cell Electroporation

The resuspended cells were transferred to an electroporation cuvette, after which 10 μg RNA was added and thoroughly mixed. The mixture was allowed to equilibrate at room temperature for 2 minutes prior to electroporation under the specified conditions. Post-electroporation, the cells were incubated in complete medium supplemented with 10% FBS for 4 hours to promote cell adherence. Subsequently, the supernatant was carefully aspirated, and the cells were gently washed with PBS to eliminate non-adherent cells. Fresh medium or appropriate treatments were then added as required.

3. Results

3.1. In Vitro Cytotoxicity and Chick Embryo Toxicity of SQXA-12

To evaluate the cytotoxicity of SQXA-12 (Figure 1), an MTT assay was performed to assess its cytotoxic effects on Vero cells, yielding a CC_{50} value of 122.98 μM (Figure 2A). Additionally, the in vivo toxicity of SQXA-12 was evaluated using SPF chicken embryos. Various doses of SQXA-12 (600, 300, 150, 75, and 37.5 μg) were administered via air sac inoculation to 10-day-old SPF chicken embryos. After a 20-day observation period, no mortality was observed among the treated embryos. Upon examination post-shell-breaking, embryos treated with doses ranging from 37.5 to 600 μg exhibited developmental characteristics comparable to those in the DMSO control group, with no significant differences noted (Figure 2B). These findings indicate that SQXA-12 is non-toxic to chicken embryos at doses ranging from 37.5 to 600 μg per embryo.

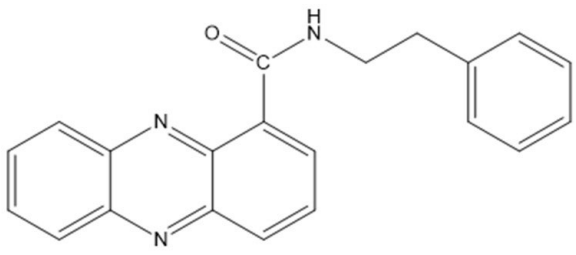

N-phenethylphenazine-1-carboxamide

Figure 1. The chemical structural formula of SQXA-12.

 doi:10.20944/preprints202503.1058.v1

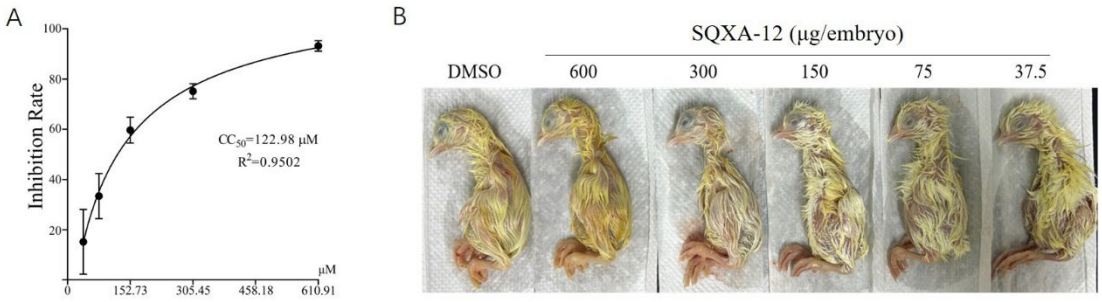

Figure 2. The cytotoxicity of SQXA-12 on Vero cells and chicken embryos. (A) Cytotoxic effects of SQXA-12 on Vero cells: Vero cells were cultured to 50% confluence and subsequently exposed to varying concentrations of SQXA-12. Once the control group reached 90% confluence, the culture medium was replaced with FBS-free DMEM. Cell viability was assessed using the MTT assay, and the 50% cytotoxic concentration (CC_{50}) of SQXA-12 was determined. Data represent the mean ± SD from three independent experiments. (B) Toxicity of SQXA-12 on chicken embryos: Fifteen10-day-old SPF chicken embryos were grouped into 3 groups, and injected via the air sac with 600, 300, 150, 75, and 37.5 μg of SQXA-12, respectively. Embryonic development was monitored for 20 days post-injection.

3.2. SQXA-12 Inhibited IBV Replication

A luciferase reporter assay was utilized to evaluate the anti-IBV efficacy of SQXA-12. Vero cells were infected with IBV-Luc, and relative luciferase activity served as an indicator of IBV-Luc protein synthesis. As illustrated in Figure 3A, the EC_{50} value of SQXA-12 was determined to be approximately 12.25 μM (equivalent to 4.01 μg/mL), based on the relative fluorescence units (RFU). Additionally, we assessed the survival rates of H1299, Vero, and DF-1 cells following treatment with SQXA-12 at concentrations of 49.00, 24.50, 12.25, 6.12, and 3.06 μM. The results indicated that the survival rates of H1299, Vero, and DF-1 cells remained above 94%, except for those treated with 24.50 μM SQXA-12, which exhibited a reduced survival rate (Figure 3B). Unless otherwise specified, the final concentration of SQXA-12 treatment mentioned in this article is 12.25 μM.

To investigate the impact of SQXA-12 on IBV replication, H1299 cells were infected with IBV-p65 at a multiplicity of infection (MOI) of 1.0 for 2 hours and subsequently treated with 12.25 μM SQXA-12. Cell samples were collected at specified time points post-infection (hpi) for quantitative detection of viral negative-strand genomic (g) RNA and subgenomic (sg) RNA synthesis by RT-qPCR. The data revealed that continuous treatment with SQXA-12 significantly reduced viral RNA accumulation during IBV-p65 infection in a time-dependent manner (Figure 3C-3D).

To further analyze the dynamics of SQXA-12's effect on IBV-p65 replication, media and cell lysates were collected at designated time points. Viral titers in these samples were measured using a plaque assay, and virus growth curves were plotted. The results demonstrated that the viral titer in both media and cell lysates peaked at 24 hpi in the absence of SQXA-12 treatment, while SQXA-12 treatment resulted in a delayed peak of viral titer. Moreover, SQXA-12 treatment led to a reduction of approximately 100-fold in viral titer at 24 hpi (Figure 3E), indicating that SQXA-12 could substantially inhibit viral growth.

 doi:10.20944/preprints202503.1058.v1

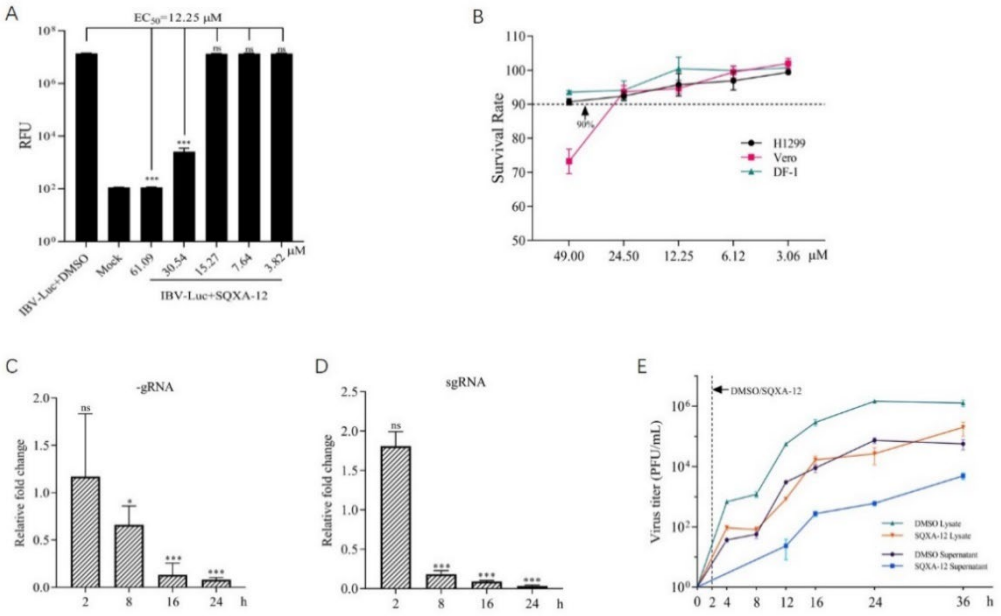

Figure 3. Inhibitory effect of SQXA-12 on IBV replication. (A) EC_{50} determination. Vero cells were infected with IBV-Luc at an MOI of 1.0 for 2 h, then treated with SQXA-12 at various concentrations in FBS-free DMEM. Cells were harvested 24 h post-infection for luciferase assay to determine the EC_{50} value. (B) Cell survival rates. H1299, Vero, and DF-1 cells were treated with 12.25 μM SQXA-12, and survival rates were measured by MTT assay. (C-D) Inhibition of IBV RNA synthesis. H1299 cells infected with IBV at an MOI of 1.0 for 2 h were treated with 12.25 μM SQXA-12. Total RNA was extracted at indicated time points for real-time RT-PCR analysis of viral (-) RNA and sgRNA. (E) Effect on IBV replication. Infected H1299 cells were treated with 12.25 μM SQXA-12, and viral growth curves were determined by plaque assay at indicated time points. Data represent mean ± SD from three independent experiments. *, P<0.05; ***, P<0.001.

3.3. SQXA-12's Precursors Had No Anti-IBV Activity

SQXA-12 is synthesized from PCA and 2-phenethylamine. To investigate whether the anti-IBV activity of SQXA-12 can be attributed to its precursors, Vero cells at 90% confluence were infected with IBV-Luc at an MOI of 1.0 for 2 hours and subsequently, varying concentrations of PCA and 2-phenethylamine were added individually. Cell lysates were collected 24 hours post-infection for luciferase activity analysis. The results indicated that PCA and 2-phenethylamine exhibited anti-IBV activities only at concentrations of 891.98 μM (Figure 4A) and 165 μM (Figure 4B), respectively, but not at lower concentrations. These concentrations are significantly higher than those required for SQXA-12 to exhibit anti-IBV activity (Figure 3A). Therefore, these findings suggest that the anti-IBV activity observed at 12.25 μM SQXA-12 is intrinsic to SQXA-12 itself rather than being attributable to PCA or 2-phenethylamine.

 doi:10.20944/preprints202503.1058.v1

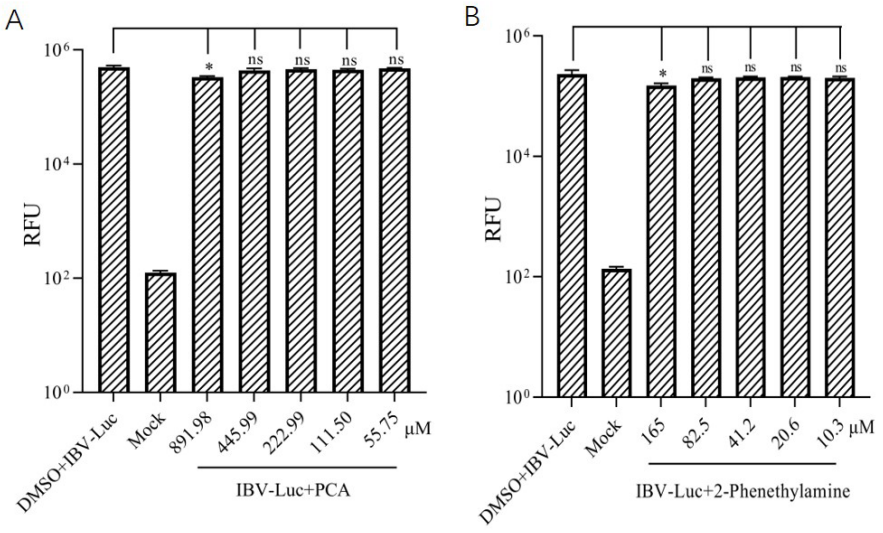

Figure 4. Anti-IBV activity of phenazine-1-carboxylic acid and β-phenethylamine. Vero cells (90% confluence) were infected with IBV-Luc at an MOI of 1.0 for 2 hours. The medium was then replaced with FBS-free DMEM, and cells were treated with phenazine-1-carboxylic acid (A) or β-phenethylamine (B) at various concentrations. At 24 hours post-infection, cells were harvested for a luciferase assay. Data represent the mean ± SD from three independent experiments. *, P<0.05.

3.4. SQXA-12 Inhibits the Expression of IBV N Protein

To analyze the effect of SQXA-12 on the expression of IBV-N in different cell lines, DF-1, H1299 and Vero cells were treated with 12.25 μM SQXA-12 at 2 hours after rIBV infection, and cell lysates were collected at the specified time points for Western blotting. The results demonstrated that SQXA-12 exerted varying degrees of inhibition on the expression of IBV-N across three cell lines. The most pronounced inhibitory effect was observed in Vero cells, where the N protein became nearly undetectable 16 to 32 hours post-infection. In H1299 cells, a faint band emerged at 16 hours post-infection, with the inhibitory efficacy diminishing as infection time progressed. In DF-1 cells, significant inhibition was noted from 6 to 32 hours post-infection (Figure 5A).

To evaluate the impact of application timing on inhibitory efficacy, rIBV-infected H1299 cells at 2, 8, 16, and 24 hours post-infection were treated with 12.25 μM SQXA-12, respectively, were harvested 32 hours post-infection, and the expression levels of the N protein were assessed via Western blot analysis. The results indicated that, compared to the control group, N protein expression was significantly reduced at 2 and 8 hours post-infection, with the most pronounced effect observed at 2 hours. In contrast, minimal changes in N protein expression were detected at 16 and 24 hours post-infection (Figure 5B). These findings suggest that effective inhibition of viral replication is only achieved when SQXA-12 is administered during the early stages of infection.

To assess the inhibitory efficacy of SQXA-12 on IBV-M41 replication, IBV-M41, together with corresponding concentrations of SQXA-12, was inoculated into 12-day-old SPF chicken embryos, and allantoic fluid was collected 48 hours post-inoculation. Western blot analysis revealed that doses of 300 and 600 μg of SQXA-12 per embryo reduced significantly the expression of N protein (Figure 5C), implying that SQXA-12 could suppress effectively IBV-M41 replication in chicken embryo.

 doi:10.20944/preprints202503.1058.v1

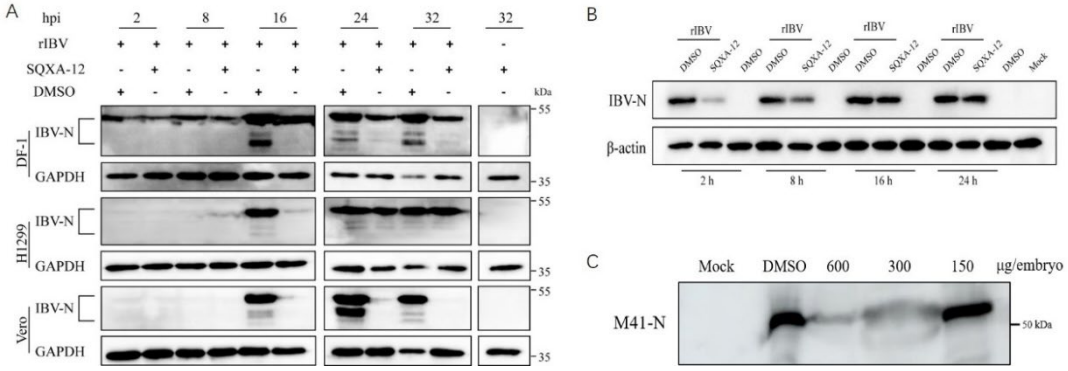

Figure 5. Inhibitory effect of SQXA-12 on IBV-N expression. (A) SQXA-12's effect on IBV-N expression in DF-1, H1299, and Vero cells. Cells were infected with rIBV (MOI=1.0) for 2 h, then treated with SQXA-12 (12.25 μM). Samples were collected at specified time point for Western blotting. (B) SQXA-12's effect on IBV-N expression in H1299 cells at different treatment times. SQXA-12 was added 2, 8, 16, and 24 h post-infection, and cells were harvested at 32 h for Western blotting. (C) SQXA-12's effect on IBV-M41 N protein expression. SPF chicken embryos (12-day-old) were co-inoculated with IBV-M41 SQXA-12 into the allantoic fluid. Fluid was collected 48 h later for Western blotting using an anti-IBV-N antibody.

3.5. Antiviral Activity of SQXA-12 Against Other RNA Viruses

Subsequently, we aimed to investigate whether SQXA-12 exhibits broad-spectrum antiviral activity. To this end, GFP-tagged VSV (GFP-VSV) was utilized to infect Vero cells, following treatment of 12.25 μM SQXA-12 at 2 hours post -infection. The expression levels of GFP were monitored at multiple time points to evaluate the replication dynamics of GFP-VSV in Vero cells. The results demonstrated that SQXA-12 effectively inhibited GFP-VSV replication (Figure 6A). Similarly, the antiviral efficacy of SQXA-12 against PRRSV, NDV, HCoV-OC43, and PEDV and was assessed using appropriate cell lines (PRRSV in Marc-145 cells, NDV in HeLa cells, HCoV-OC43 and PEDV in H1299 cells). Western blot analysis revealed that SQXA-12 suppressed the replication of these viruses in their respective host cells, albeit to varying degrees (Figure 5B-5E). Additionally, AIV-H9N2 and corresponding concentrations of SQXA-12 were co-inoculated into 14-day-old SPF chicken embryos. After a 72-hour incubation period, allantoic fluid was harvested, and hemagglutination assays were performed to quantify AIV-H9N2 hemagglutinin (HA) protein expression. The findings indicated that hemagglutination occurred at dilutions of 2^{-6} in both the control group and the 150 μg dose group, while no hemagglutination was observed at any dilution in the 300 μg dose group (Figure 6F), suggesting that AIV-H9N2 replication was significantly restricted.

 doi:10.20944/preprints202503.1058.v1

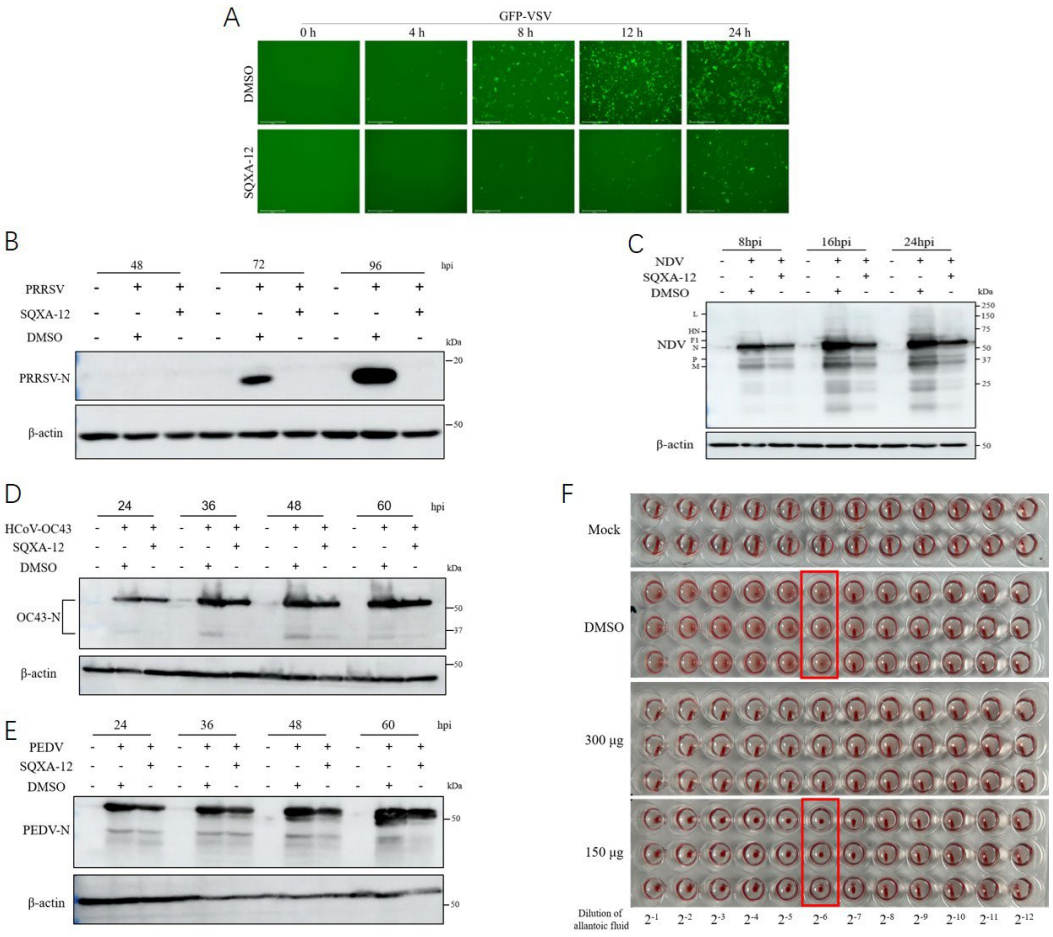

Figure 6. Antiviral activities of SQXA-12 on various RNA viruses. (A) For GFP-VSV, SQXA-12 was added to Vero cells 2 hours post-infection, and GFP expression was observed under a fluorescence microscope at specified time points. (B) For PRRSV, (C) NDV, (D) HCoV-OC43, and (E) PEDV, SQXA-12 was added post-infection, and cell lysates were collected for Western blotting at indicated times. (F) For AIV-H9N2, SQXA-12 was co-inoculated with the virus into 14-day-old SPF chicken embryos. After 72 hours, allantoic fluid was collected for hemagglutination assays.

Taken together, these findings indicate that SQXA-12 exerts an inhibitory effect on the replication of both positive-sense and negative-sense RNA viruses.

3.6. SQXA-12 Imposes Restrictions on the Replication of IBV-p65 RNA

The genomic RNA of IBV is inherently infectious. To evaluate the direct impact of SQXA-12 on viral RNA replication, total RNA extracted from IBV-p65-infected H1299 cells at 24 hours post-infection was electroporated into H1299 cells under conditions of 150 V and 20 ms. Cells were subsequently treated with concentrations of 24.5 μM, 12.25 μM, and 6.125 μM of SQXA-12, and samples were collected after an additional 24-hour incubation period. Western blot analysis was employed to assess the expression levels of the N protein. The results indicated that treatment with 12.25 μM and 6.125 μM of SQXA-12 significantly inhibited intracellular expression of the N protein derived from IBV-p65 RNA (Figure 7).

 doi:10.20944/preprints202503.1058.v1

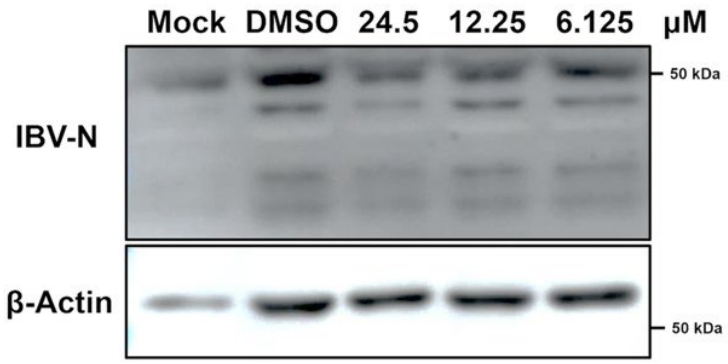

Figure 7. SQXA-12 restricted the replication of IBV-p65 RNA. 10 μg total RNA extracted from IBV-p65-infected H1299 cells at 24 h.p.i was electroporated into H1299 cells under the 150 V/20 ms condition. The cells were treated with 24.5, 12.25, and 6.125 μM of SQXA-12, and samples were collected after 24 hours. Western blotting was used to evaluate the expression of the N protein.

4. Discussion

In this study, we identified a novel compound, SQXA-12, from a series of synthesized phenazinamide derivatives and demonstrated its potent antiviral activity against IBV. Experimental results indicated that SQXA-12 exhibited a CC_{50} value of approximately 122.98 μM for Vero cells, with no significant toxicity observed in chicken embryos at concentrations ranging from 37.5 to 600 μg (Figure 2). Furthermore, the EC_{50} of SQXA-12 against IBV was determined to be 12.25 μM (Figure 3A), at which point the survival rates of Vero and H1299 cells were maintained at above 94%, and it was non-toxic to DF-1 cells (Figure 3B). Subsequent experiments revealed that SQXA-12 at a final concentration of 12.25 μM treating cells infected with IBV for 2 hours significantly inhibited IBV RNA synthesis (Figure 3C-3D) and N protein expression (Figure 5A-5B). This inhibitory effect persisted in Vero and DF-1 cells up to 32 hours post-infection, suggesting potential therapeutic efficacy of SQXA-12 against IBV. Additionally, SQXA-12 at concentrations of 300 and 600 μg per embryo effectively suppressed IBV-M41 replication in embryonated eggs (Figure 5C). Moreover, our research indicates that SQXA-12 at 12.25 μM exhibited varying degrees of in vitro antiviral activity against a range of negative-sense RNA viruses (e.g., VSV, NDV) and positive-strand RNA viruses (e.g., PRRSV, HCoV-OC43, PEDV). Notably, the most pronounced inhibitory effect was observed against PRRSV, where N protein was undetectable 90 hours post-infection (Figure 6A-6E), suggesting its potential efficacy in controlling the PRRSV-induced disease. Hemagglutination assays further confirmed that SQXA-12 at 300 and 600 μg per chicken embryo effectively inhibited the replication of avian influenza virus H9N2 in embryonated eggs (Figure 6F). Considering that these viruses belong to distinct families or genera, it is reasonable to infer that SQXA-12 exhibits broad-spectrum antiviral activity against both positive-strand and negative-strand RNA viruses. Given that IBV-M41, NDV, and AIV-H9N2 are all capable of infecting chickens, it is plausible to consider the potential of a single therapeutic agent, SQXA-12, for the prevention and control of these three viruses.

The replication of RNA viruses is mediated by a virus-encoded RNA-dependent RNA polymerase (RdRp), which precisely orchestrates the polymerization process at specific loci, an essential step for accurate viral replication [18,19]. Importantly, the RdRp core region exhibits high conservation across diverse RNA virus species, rendering it a promising target for antiviral drug development. Several antiviral drugs utilized in the clinical management of COVID-19 inhibit viral replication by targeting RdRP [6,10,20]. Our electroporation experiments with IBV RNA demonstrated that SQXA-12 exerts its inhibitory effect during the replication or expression phase of IBV RNA. Whether SQXA-12 can directly inhibit RdRp activity is under investigation.

In summary, our study identifies SQXA-12 as a promising therapeutic agent for the clinical management of IBV. SQXA-12 may be particularly well-suited for post-infection therapeutic applications. Furthermore, a thorough investigation into the broad-spectrum antiviral mechanisms

 doi:10.20944/preprints202503.1058.v1

of SQXA-12 is warranted to elucidate its molecular targets, which could pave the way for its potential use as a novel drug in future strategies to combat IBV and other RNA viral pandemics.

Author Contributions: Cai Z. assisted in the design, performed experiments, analysis and interpretation of data, and drafted manuscript; Zhang M. performed partial experiments; Li J. and Wu Q. designed and synthesized SQXA-12; Liu D.X. designed experiments, provided cell lines and viruses, and edited draft; Fang S. designed experiments, review and editing, project administration, and funding acquisition. All authors have read and agreed to the published version of the manuscript.

Funding Statement: This work was financially supported by grants from the National Natural Science Foundation of China (No. 31572490).

Acknowledgments: We sincerely acknowledgment Dr. Liu D.X. for providing Mac-15 cell line, HCoV-OC43, PEDV, NDV, PRRSV, and AIV-H9N2. We also particularly acknowledgment Dr. Weng C.J. for providing GFP-VSV.

Conflicts of Interest: The authors declare no conflicts of interest.

References

1. Cui, J.; Li, F.; Shi, Z.L. Origin and evolution of pathogenic coronaviruses. Nat Rev Microbiol. 2019; 17(3): 181-192
2. Falchieri, M.; Coward, V.J.; Reid, S.M.; Lewis, T.; Banyard, A.C. Infectious bronchitis virus: an overview of the “chicken coronavirus”. J Med Microbiol. 2024; 73(5): 001828.
3. Bande, F.; Arshad, S.S.; Omar, A.R.; Hair-Bejo, M.; Mahmuda, A.; Nair, V. Global distributions and strain diversity of avian infectious bronchitis virus: a review. Anim Health Res Rev. 2017; 18(1): 70-83.
4. Jordan, B. Vaccination against infectious bronchitis virus: A continuous challenge. Vet Microbiol. 2017; 206:137-143.
5. Rohaim, M.A.; El Naggar, R.F.; Abdelsabour, M.A.; Mohamed, M.H.A.; El-Sabagh, I.M.; Munir, M. Evolutionary analysis of infectious bronchitis virus reveals marked genetic diversity and recombination events. Genes (Basel). 2020; 11(6): 605.
6. Yu, B.; Chang, J. The first Chinese oral anti-COVID-19 drug Azvudine launched. Innovation (Camb). 2022; 3(6): 100321
7. Gentile, I.; Scotto, R.; Schiano Moriello, N.; Pinchera, B.; Villari, R.; Trucillo, E.; Ametrano, L.; Fusco, L.; Castaldo, G.; Buonomo, A.R.; & Federico Ii Covid Team. Nirmatrelvir/Ritonavir and Molnupiravir in the treatment of mild/moderate COVID-19: Results of a real-life study. Vaccines, 2022; 10(10), 1731.
8. Wong, C.K.H.; Au, I.C.H.; Lau, K.T.K.; Lau, E.H.Y.; Cowling, B.J.; Leung, G.M. Real-world effectiveness of molnupiravir and nirmatrelvir plus ritonavir against mortality, hospitalisation, and in-hospital outcomes among community-dwelling, ambulatory patients with confirmed SARS-CoV-2 infection during the omicron wave in Hong Kong: an observational study. Lancet (London, England), 2022, 400(10359), 1213–1222.
9. Li, G.; Hilgenfeld, R.; Whitley, R.; De Clercq, E. Therapeutic strategies for COVID-19: progress and lessons learned. Nat Rev Drug Discov. 2023; 22(6): 449-475.
10. Kumar, M.; Baig, M.S.; Bhardwaj, K. Advancements in the development of antivirals against SARS-Coronavirus. Front Cell Infect Microbiol. 2025; 15: 1520811.
11. Mavrodi, D.V.; Blankenfeldt, W.; Thomashow, L.S. Phenazine compounds in fluorescent , *Pseudomonas spp.* biosynthesis and regulation. Annu Rev Phytopathol. 2006; 44:417-45.
12. Biessy, A.; Filion, M. Phenazines in plant-beneficial Pseudomonas spp.: biosynthesis; regulation; function and genomics. Environ Microbiol. 2018; 20(11): 3905-3917.
13. Qin, C.; Yu, D.Y.; Zhou, X.D.; Zhang, M.; Wu, Q.L.; Li, J.K. Synthesis and antifungal evaluation of PCA amide analogues. J Asian Nat Prod Res. 2019; 21(6): 587-596.
14. Palchykovska, L.G.; Vasylchenko, O.V.; Platonov, M.O.; Kostina, V.G.; Babkina, M.M.; Tarasov, O.A.; Starosyla, D.B.; Samijlenko, S.P.; Rybalko, S.L.; Deriabin, O.M.; Hovorun, D.M. Evaluation of antibacterial

 doi:10.20944/preprints202503.1058.v1

and antiviral activity of N-arylamides of 9-methyl and 9-methoxyphenazine-1-carboxylic acids- inhibitors of the phage T7 model transctiption. Biopolym Cell. 2012; 28(6): 477-485.

15. Fang, S.; Chen, B.; Tay, F.P.; Ng, B.S.; Liu, D.X. An arginine-to-proline mutation in a domain with undefined functions within the helicase protein (Nsp13) is lethal to the coronavirus infectious bronchitis virus in cultured cells. Virology. 2007; 358(1): 136-47.
16. Shen, H.; Fang, S.G.; Chen, B.; Chen, G.; Tay, F.P.; Liu, D.X. Towards construction of viral vectors based on avian coronavirus infectious bronchitis virus for gene delivery and vaccine development. J Virol Methods. 2009; 160(1-2): 48-56.
17. An, H.; Cai, Z.; Yang, Y.; Wang, Z.; Liu, D.X.; Fang, S. Identification and formation mechanism of a novel noncoding RNA produced by avian infectious bronchitis virus. Virology. 2019; 528: 176-180.
18. den Boon, J.A.; Nishikiori, M.; Zhan, H.; Ahlquist, P. Positive-strand RNA virus genome replication organelles: structure, assembly, control. Trends Genet. 2024; 40(8): 681-693.
19. Xue, L.; Chang, T.; Li, Z.; Wang, C.; Zhao, H.; Li, M.; Tang, P.; Wen, X.; Yu, M.; Wu, J.; Bao, X.; Wang, X.; Gong, P.; He, J.; Chen, X.; Xiong, X. Cryo-EM structures of Thogoto virus polymerase reveal unique RNA transcription and replication mechanisms among orthomyxoviruses. Nat Commun. 2024;15(1): 4620.
20. Cao, Z.; Gao, W.; Bao, H.; Feng, H.; Mei, S.; Chen, P.; Gao, Y.; Cui, Z.; Zhang, Q.; Meng, X.; Gui, H.; Wang, W.; Jiang, Y.; Song, Z.; Shi, Y.; Sun, J.; Zhang, Y.; Xie, Q.; Xu, Y.; Ning, G.; Gao, Y.; Zhao, R. VV116 versus nirmatrelvir-ritonavir for oral treatment of Covid-19. N Engl J Med. 2023; 388(5): 406-417.